



Published in final edited form as:

*Chem Res Toxicol.* 2017 April 17; 30(4): 1102–1110. doi:10.1021/acs.chemrestox.7b00009.

## Oncometabolites D- and L-2-hydroxyglutarate Inhibit the AlkB Family DNA Repair Enzymes under Physiological Conditions

Fangyi Chen<sup>†,‡</sup>, Ke Bian<sup>†,‡</sup>, Qi Tang<sup>†</sup>, Bogdan I. Fedeles<sup>⊥,§,‡</sup>, Vipender Singh<sup>⊥,§,‡</sup>, Zachary T. Humulock<sup>†</sup>, John M. Essigmann<sup>⊥,§,‡</sup>, and Deyu Li<sup>\*,†</sup>

<sup>†</sup>Department of Biomedical and Pharmaceutical Sciences, College of Pharmacy, University of Rhode Island, Kingston, Rhode Island 02881, United States

<sup>⊥</sup>Department of Biological Engineering, Massachusetts Institute of Technology, Cambridge, Massachusetts 02139, United States

<sup>§</sup>Department of Chemistry, Massachusetts Institute of Technology, Cambridge, Massachusetts 02139, United States

<sup>‡</sup>Center for Environmental Health Sciences, Massachusetts Institute of Technology, Cambridge, Massachusetts 02139, United States

### Abstract

Cancer-associated mutations often lead to perturbed cellular energy metabolism and accumulation of potentially harmful oncometabolites. One example is the chiral molecule 2-hydroxyglutarate (2HG); its two stereoisomers (D- and L-2HG) have been found with abnormally high concentrations in tumors featuring anomalous metabolic pathways. 2HG has been demonstrated to competitively inhibit several  $\alpha$ -ketoglutarate ( $\alpha$ KG)- and non-heme iron-dependent dioxygenases, including some of the AlkB family DNA repair enzymes, such as ALKBH2 and ALKBH3. However, previous studies have only provided the IC<sub>50</sub> values of D-2HG on the enzymes and the results have not been correlated to physiologically relevant concentrations of 2HG and  $\alpha$ KG in cancer cells. In this work, we carried out detailed kinetic analyses of DNA repair reactions catalyzed by ALKBH2, ALKBH3 and the bacterial AlkB in the presence of D- and L-2HG in both double and single stranded DNA contexts. We determined kinetic parameters of inhibition, including  $k_{cat}$ ,  $K_M$ , and  $K_i$ . We also correlated the relative concentrations of 2HG and  $\alpha$ KG previously measured in tumor cells with the inhibitory effect of 2HG on the AlkB family enzymes. Both D- and L-2HG significantly inhibited the human DNA repair enzymes ALKBH2 and ALKBH3 under pathologically relevant concentrations (73–88% for D-2HG and 31–58% for L-2HG inhibition). This work provides a new perspective that the elevation of either D- or L-2HG

\*Corresponding Author, Mailing address: 7 Green House Road, Pharmacy Building, Room 495 N, Kingston, Rhode Island 02881, United States. Phone number: (401) 874-9361, deyuli@uri.edu.

Present Address: Novartis Institute of Biomedical Research, Cambridge, Massachusetts 02139, United States

<sup>‡</sup>T.C. and K.B. contributed equally to this work.

### ASSOCIATED CONTENT

#### Supporting Information

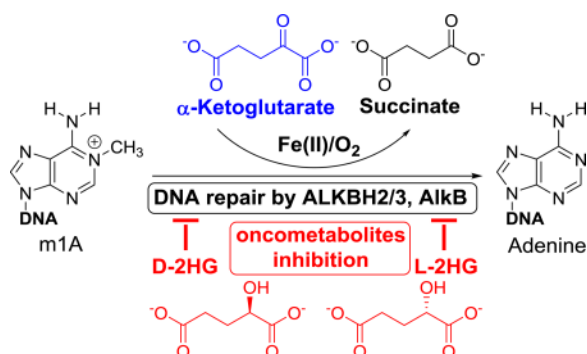
The Supporting Information is available free of charge on the ACS Publications website at DOI: XXX.

Tables of molecular weights and m/z values, initial rate for kinetic studies, and IC<sub>50</sub> values of inhibition reactions; figures for steady-state kinetics, repair percentage of reactions, and inhibition curves of different repair enzymes (PDF)

The authors declare no competing financial interest.

in cancer cells may contribute to an increased mutation rate by inhibiting the DNA repair carried out by the AlkB family enzymes and thus exacerbate the genesis and progression of tumors.

## Abstract



## Keywords

2-hydroxyglutarate; oncometabolite; ALKBH2; ALKBH3; AlkB; DNA repair inhibition; tumorigenesis

## INTRODUCTION

Mutations in the isocitrate dehydrogenases 1 and 2 (IDH1 and IDH2) are frequently found in >75% human low grade glioma, secondary glioblastoma, cartilaginous tumor and >20% of acute myeloid leukemia.<sup>1–5</sup> Tumor-derived mutant forms of IDH catalyze the NAD-dependent dehydrogenation of  $\alpha$ -ketoglutarate ( $\alpha$ KG) to D-2-hydroxyglutarate (D-2HG), a function that supplants the physiological activity of IDH, which entails reductive decarboxylation of isocitrate to  $\alpha$ KG (Figure 1b).<sup>6–13</sup> L-2HG, the stereoisomer of D-2HG, has been identified as an oncometabolite with elevated concentrations in renal cell carcinoma<sup>9,10</sup> neurodegenerative disorders,<sup>14,15</sup> and in tissues under oxygen limitation or hypoxic conditions.<sup>11,12</sup> The elevation of L-2HG under such conditions is key from either loss of expression of L-2HG dehydrogenase or promiscuous substrate utilization by lactate dehydrogenase A and malate dehydrogenases 1 and 2.<sup>10,12</sup> Both D-2HG (R-2HG) and L-2HG (S-2HG) and several other molecules have been identified as oncometabolites because their accumulations in different tumor cells are originated from dysregulated energy metabolism pathways and metabolic imbalance.<sup>16–20</sup> Because of their structural similarity to  $\alpha$ KG, both D- and L-2HG could compete with  $\alpha$ KG and inhibit enzymatic processes that use  $\alpha$ KG as a substrate. One important class of enzymes that utilizes  $\alpha$ KG—and thus potentially susceptible to inhibition by 2HG—is the non-heme iron- and  $\alpha$ KG-dependent dioxygenases, a family of enzymes with over 80 different members.<sup>21–24</sup> 2HG has been demonstrated to inhibit several  $\alpha$ KG-dependent enzymes, such as histone demethylases, prolyl hydroxylases, the TET family 5-methylcytosine (5mC) hydroxylases,<sup>7</sup> and some of the AlkB family DNA repair enzymes, such as ALKBH2 and ALKBH3.<sup>8,25</sup> However, in the case of the AlkB proteins, previous *in vitro* studies have only provided the IC<sub>50</sub> values of 2HG on the enzymes and the results have not been extrapolated to physiologically relevant

concentrations of 2HG and  $\alpha$ KG in cancer cells. While Wang et al. demonstrated that the accumulation of DNA damage in cells producing high levels of D-2HG is consistent with inhibition of ALKBH2 and/or ALKBH3,<sup>25</sup> the detailed mechanism of inhibition of the AlkB enzymes by 2HG has not been reported. A careful study of the inhibitory effect of both D- and L-2HG on AlkB repair enzymes is needed to quantify the extent of inhibition of the direct reversal DNA repair pathways; perturbations in these pathways would lead to unrepaired mutagenic DNA lesions, which would cause mutations that can accelerate tumor progression or enable metastatic growth. Such a study would also facilitate the identification of druggable targets related to the AlkB enzymes because many alkylating chemotherapeutic agents generate DNA adducts that are repaired by this family of repair enzymes.<sup>26</sup> Inhibition of these enzymes would thus afford a clinical benefit in anti-tumor regimens.

The *Escherichia coli* AlkB protein was discovered to be an  $\alpha$ KG/Fe(II)-dependent dioxygenase that oxidizes the alkyl groups in DNA adducts formed by alkylation agents, ultimately restoring the undamaged DNA bases (Figure 1a).<sup>27–29</sup> Nine human homologs of AlkB have been identified as ALKBH1–8 and FTO.<sup>29,30</sup> Among these homologs, ALKBH2<sup>31–36</sup> and ALKBH3<sup>37–40</sup> have been identified as major DNA repair enzymes for repairing small alkyl DNA lesions. Since the initial discovery of the catalytic mechanism of AlkB in 2002,<sup>27,28</sup> a range of alkyl adducts have been identified as substrates for AlkB, ALKBH2 and ALKBH3, both *in vitro* and *in vivo*.<sup>24</sup> The adducts include all of the seven N-methyl adducts occurring at the Watson-Crick (W-C) base-pairing face of the four nucleobases.<sup>41</sup> The seven adducts include 3-methylcytosine (m3C),  $N^4$ -methylcytosine, 1-methyladenine (m1A),  $N^6$ -methyladenine, 3-methylthymine, 1-methylguanine, and  $N^2$ -methylguanine. AlkB has also been reported to repair other DNA adducts, such as 1,  $N^6$ -ethenoadenine, 1,  $N^6$ -ethenoadenine, 3,  $N^4$ -ethenocytosine, 3-ethylcytosine, 1,  $N^2$ -ethenoguanine, 3,  $N^4$ - $\alpha$ -hydroxyethanocytosine, 3,  $N^4$ - $\alpha$ -hydroxypropanocytosine,  $N^2$ -ethylguanine,  $N^2$ -tetrahydrofuran-2-yl-methylguanine,  $N^2$ -furan-2-yl-methylguanine, malondialdehyde-guanine,  $\alpha$ -hydroxypropanoguanine, and  $\gamma$ -hydroxypropanoguanine.<sup>41–49</sup> The repair efficiency and substrate scope of the AlkB family enzymes have been recently reviewed in detail.<sup>24,30,50–54</sup>

In this work, we carried out kinetic analyses of DNA repair reactions catalyzed by ALKBH2, ALKBH3 and AlkB in the presence of the inhibitors D- and L-2HG. Oligonucleotides containing the methylated bases m1A and m3C were selected as substrates for the repair reactions because they are most efficiently repaired by these three enzymes.<sup>24</sup> For each substrate/enzyme/inhibitor combination, we determined a complete panel of kinetic parameters, ( $k_{cat}$ ,  $K_M$ ,  $k_{cat}/K_M$ ,  $K_i$ ), and correlated the relative concentrations of 2HG and  $\alpha$ KG found in tumor cells with the inhibitory effect of 2HG on the AlkB family enzymes. Because ALKBH2 preferentially repairs adducts in double stranded (ds) DNA and ALKBH3 prefers to repair lesions in a single stranded (ss) DNA context, we tested the three repair enzymes with both ds and ss DNA substrates. This is the first report of 2HG inhibition of AlkB family DNA repair evaluated in both single- and double- stranded DNA. We also developed an HPLC-based method to study DNA repair in the ds-DNA. The results showed that both ALKBH2 and ALKBH3, the major mammalian direct reversal repair enzymes for alkylated DNA damage, were significantly inhibited by D- and L-2HG under pathophysiologically relevant conditions.

## EXPERIMENTAL PROCEDURES

### Oligonucleotide Synthesis

Sixteen-mer oligonucleotides were synthesized with the sequence 5'-GAAGACCTXGGCGTCC-3' containing the lesions m1A and m3C at the X position.<sup>43,55</sup> The complementary 23mer oligonucleotides were synthesized with the sequence of 5'-CTGGGACGCCYAGGTCTTCACTG-3', where Y represents the position incorporating the regular bases T or G, and named as 23mer-Tcp or 23mer-Gcp. The 23mer oligonucleotides complementary to 23mer-Tcp and 23mer-Gcp were also synthesized, with the sequence 5'-CAGTGAAGACCTZGGCGTCCCAG-3', where Z was the regular base A or C, named as 23mer-A or 23mer-C. All DNA syntheses employed solid-phase phosphoramidite chemistry performed on a MerMade-4 Oligonucleotide Synthesizer.<sup>55</sup> The oligonucleotides were purified by HPLC (Thermo Fisher Scientific) on a DNAPac PA-100 Semi-Preparative column (Phenomenex). Solvent A was 100 mM 1:1 triethylamine-acetic acid (TEAA) in water and solvent B was 100% acetonitrile. The concentration of DNA was determined by UV absorbance at 260nm by NanoDrop. The oligonucleotides were characterized by HPLC-electrospray ionization triple quadrupole time of flight mass spectrometry (AB Sciex) (Table S1).

### Expression and Purification of the AlkB, ALKBH2 and ALKBH3 Proteins

ALKBH2, ALKBH3 and AlkB were expressed and purified as described and shown previously.<sup>47,55</sup> In the following section, AlkB is used as an example to illustrate the purification protocols. Briefly, His-tagged AlkB was obtained by transforming pET28a-AlkB into *E. coli* Rosetta2(DE3)pLysS or BL21(DE3)pLysS cells and protein expression was induced by the addition of 1mM isopropyl-b-D-thiogalactopyranoside (IPTG) at 37 °C (37 °C for ALKBH2 and 30 °C for ALKBH3). The expressed protein was purified by affinity chromatography. Thrombin was used to digest His-tag containing AlkB protein. The final purified protein was stored -80 °C in AlkB storage buffer as previously described.<sup>55</sup>

### Enzymatic Reaction

To assay the AlkB family demethylase activity toward the two substrates in ss- and ds-DNA, the enzymatic reactions were performed at 37 °C at different time points for the kinetic study of the AlkB reaction in buffer [70.0 μM Fe(NH<sub>4</sub>)<sub>2</sub>(SO<sub>4</sub>)<sub>2</sub>·6H<sub>2</sub>O, 0.93 mM α.KG (0.1 mM for 2-HG inhibition assay), 1.86 mM ascorbic acid and 46.5 mM HEPES (pH 8.0)]. The reactions were stopped by adding 10 mM EDTA followed by heating at 95 °C for 5 min. Typically, the purified proteins were incubated with oligonucleotides containing DNA adducts in the presence of all cofactors in a 20 μL reaction volume. In order to separate substrate and product, 16mer m1A and A or 16mer m3C and C, the HPLC condition started with a 5 min gradient of 1.5 M ammonium acetate from 50% to 65%, followed by 2 min 70% ammonium acetate. The column was DNAPac PA-100 (4× 250 mm) (Thermo Scientific). The UV detection wavelength was at 260 nm. Each reaction was carried out in triplicate.

For the double-stranded DNA substrates, 1.5 equivalents of the 23mer complementary oligonucleotides, 23mer-Tcp or 23mer-Gcp, were annealed with 16mer oligos by heating the

mixture at 80 °C for 10 min and then cooling down to room temperature with the rate of 1 °C/10 s. The post-reaction treatments were similar to those for the ss-DNA reactions, except 1.75 equivalents of 23mer-A and 23mer-C were added together with 10 mM EDTA followed by heating up to 95 °C for 10 min and then cooled down to room temperature with the same rate as used for annealing. The quantification method was the same as described above. Each reaction was carried out in triplicate.

### Kinetic Studies

To determine  $K_M$ ,  $k_{cat}$  and  $K_i$  values for the repair reactions, initial rates were obtained by keeping the DNA substrate and enzyme concentration constant and varying  $\alpha$ KG concentration with or without various concentrations of D- or L-2HG (0, 1.0, 3.0, 5.0, 7.0, 9.0, 37.3 mM). All reactions were performed at 37 °C in triplicate and the data were analyzed by GraphPad Prism 5 with the Michaelis-Menten kinetics model. The inhibition curves were fit to the equation:  $1/V_0 = 1/V_{max} + (K_M/V_{max}) \times (1 + [I]/K_i) \times (1/[S])$ .

## RESULTS

To test the inhibitory effect of D- and L-2HG on the AlkB family enzymes, we first chemically synthesized oligonucleotides by site-specifically incorporating m1A and m3C, the major substrates of the AlkB family enzymes.<sup>24,43</sup> We also expressed and purified recombinant human ALKBH2 and ALKBH3 proteins, and the *E. coli* AlkB protein.<sup>55</sup> Then, we performed kinetic experiments to determine the  $k_{cat}$  and  $K_M$  of the three enzymes as they repair the two adducts in both ds- and ss-DNA. After that, we measured the  $K_i$  of D- and L-2HG on the repair reactions, and finally evaluated the inhibitory effect of the oncometabolites in the concentration range reported to occur in certain human cancers.

### Oligonucleotide Synthesis and Protein Purification

Two 16mer oligonucleotides containing m1A and m3C were chemically synthesized with the sequence 5'-GAAGACCTXGGCGTCC-3' (X denotes the alkylated base).<sup>43</sup> After HPLC purification, the identity of the oligonucleotides was confirmed by comparing the theoretical  $m/z$  of the oligonucleotides with the observed  $m/z$  from high resolution LC-MS (Table S1). The genes for *E. coli* AlkB and its human homologs ALKBH2 and ALKBH3 were cloned into pET28a+ expression vector; the incorporation of the correct sequences was confirmed by sequencing the corresponding plasmids. The three proteins were then expressed in *E. coli* hosts, isolated and purified by affinity chromatography as described in Experimental Section.<sup>55</sup>

### Enzymatic Assay for Measuring Kinetic Constants

For each enzymatic reaction, the adduct-containing oligonucleotide was incubated with the necessary cofactors for the AlkB reaction: Fe(II),  $\alpha$ KG, and ascorbic acid (see Experimental Section) in either ss- or ds-DNA. Below, m1A will be used as an example to explain the HPLC analyses. For the ss-DNA reactions, the starting material 16mer m1A (1.5 min in Figure 2a) and product 16mer A (2.8 min in Figure 2b) were well separated by anion exchange HPLC, and the amount of each was quantified by reference to standard curves. For ds-DNA repair reactions, we initially used a 16mer complementary oligonucleotide.

However, the dsDNA of starting material (16mer complementary plus 16mer m1A) and the dsDNA of product (16mer complementary plus 16mer A) could not be fully separated under various HPLC conditions, thus making the quantification of reactions challenging. Therefore, we adopted a longer complementary oligonucleotide (23mer Tcp, 5.6 min in Figure 2c), which provided a similar repair efficiency as the 16mer complementary oligonucleotide. In the analysis of the 23mer reaction, the dsDNA of starting material (23mer Tcp plus 16mer m1A, 7.5min in Figure 2c) and the dsDNA of product (23mer Tcp plus 16mer A, 7.7min in Figure 2c) still could not be fully separated under the HPLC condition. Consequently, we designed another 23mer oligonucleotide that was fully complementary to 23mer Tcp (23mer A, 5.5min in Figure 2d). After the dsDNA reaction with 23mer Tcp, 23mer A was added to the reaction mixture, and the mixture was heated to 80 °C for 10 min and then slowly cooled down to room temperature. The addition of 23mer A allowed the 23mer Tcp formed perfect dsDNA with 23mer A (9.1 min in Figure 2d), thus releasing 16mer m1A and 16mer A from their previous complementarity with 23mer Tcp. Under these conditions, the 16mer m1A and 16mer A in the dsDNA repair reaction were well separated and quantified by the HPLC analyses (Figure 2d). A similar analytical strategy was successfully applied to m3C dsDNA repair reactions.

### Kinetic Analyses

After setting up a reliable procedure to quantify the conversion of the repair reactions, we carried out systematic kinetic analyses of the AlkB family enzymes repairing m1A and m3C. Because the purpose of this work was to measure the possible inhibition of D- and L-2HG on the repair reactions catalyzed by  $\alpha$ KG-dependent AlkB family enzymes, the kinetic parameters of  $\alpha$ KG in the repair reactions were first measured. In a typical kinetic analysis (e.g., ALKBH2 repairing m1A), 5  $\mu$ M of oligonucleotide substrate, and 0.2  $\mu$ M ALKBH2 enzyme were mixed with different concentrations of  $\alpha$ KG (5.0–70.0  $\mu$ M) and the extent of the repair reaction was quantified at different time points (see Experimental section for details). Because the repair of one molecule m1A to A requires the conversion of one molecule of  $\alpha$ KG to succinate (Figure 1), the concentrations of the product 16mer A were used to calculate the  $k_{\text{cat}}$  and  $K_{\text{M}}$  of  $\alpha$ KG. To ensure that the kinetic parameters reflect initial velocity, the DNA and enzyme concentrations were optimized to make sure the conversion of the repair reactions was less than 20%. All reactions were carried out in triplicate.

For ALKBH2 repair of m1A in ds-DNA (Table 1, Table S2, and Figure S1), the  $k_{\text{cat}}$  of  $\alpha$ KG was  $2.5 \pm 0.1 \text{ min}^{-1}$  and the  $K_{\text{M}}$  was  $7.3 \pm 0.9 \mu\text{M}$ , which are comparable to the literature reported kinetics parameters of other  $\alpha$ KG dependent enzymes.<sup>7,25,56–61</sup> The  $k_{\text{cat}}/K_{\text{M}}$  value of ds-repair reaction ( $0.34 \text{ min}^{-1} \cdot \mu\text{M}^{-1}$ ) shows that the repair was more efficient than in ss-DNA ( $0.28 \text{ min}^{-1} \cdot \mu\text{M}^{-1}$ ), which agrees with the literature on the reported strand preference of ALKBH2.<sup>59</sup> The kinetic data of ALKBH2 repair of m3C showed a similar trend (Table 1, Table S2, Table S4 and Figure S2). In contrast to ALKBH2's preference for ds-DNA substrates, the kinetic parameters of ALKBH3 repair of ds-DNA substrates could not be measured due to the low conversion ratio even with very high enzyme loading, such as 5.0  $\mu$ M of ALKBH3 to 5.0  $\mu$ M substrate. Conversely, ALKBH3 could efficiently repair both DNA adducts in ss-DNA (Table 1). These results confirm the previously reported preference

of ALKBH3's repair of ss-DNA substrates.<sup>48,55</sup> The kinetic factors of the *E. coli* AlkB protein were also measured and the  $k_{\text{cat}}$  and  $K_{\text{M}}$  values agreed well with the literature reported  $k_{\text{cat}}$  and  $K_{\text{M}}$  of the reactions (Table 1, Table S2 and S3, and Figure S3 and S4).<sup>59,60</sup> The  $k_{\text{cat}}/K_{\text{M}}$  values of AlkB repair confirm that the enzyme prefers to repair m1A and m3C in ss-DNA as compared with ds-DNA.<sup>55</sup>

## 2HG Inhibition of the DNA Repair Reactions Catalyzed by the AlkB Family Enzymes

With reliable  $k_{\text{cat}}$  and  $K_{\text{M}}$  parameters of the three enzymes, we set out to measure the  $K_{\text{i}}$  values of D-2HG and L-2HG together with a positive control, N-oxalylglycine (N-OG), a commonly used inhibitor of  $\alpha$ KG dependent enzymes.<sup>7</sup> Because D-2HG and L-2HG are chiral molecules, polarimetry (P-2000 Digital Polarimeter, JASCO Inc.) was utilized to measure their optical activity in a 1 decimeter cell. The optical rotation of D-2HG was  $\pm 9.5^\circ$  ( $c = 1.0$ , 0.1M NaOH), which agreed well to the value provided by the commercial source ( $[\alpha]_{\text{D}} \pm 8.5 \pm 1.5^\circ$ ,  $c = 1.0$  in NaOH, Sigma-Aldrich Co LLC). Similarly, the optical rotation of L-2HG was  $-8.0^\circ$ , which was consistent with the reported  $-8.5 \pm 1.5^\circ$  value. These values confirm the chirality and purity of the two enantiomers.

For the inhibition of the ALKBH2 repair reaction on m1A in ds- and ss-DNA, the  $K_{\text{i}}$  values for D-2HG are  $280 \pm 61 \mu\text{M}$  and  $405 \pm 61 \mu\text{M}$ , respectively (Table 2, Figure 3a and 3b, Table S5). These data indicate that D-2HG has a stronger binding affinity for the complex of ALKBH2 with ds-DNA than ss-DNA. For L-2HG reactions, the  $K_{\text{i}}$  values are similar but smaller (stronger inhibition) than with the corresponding D-2HG reactions (Table 2, Figure 3d and 3e, Table S5). The  $K_{\text{i}}$  values of N-OG show much stronger inhibition (with about 10 times more potency, Table 2) of all repair reactions with the  $K_{\text{i}}$  values ranging from 6 to 40  $\mu\text{M}$ . For the inhibition of ALKBH3, a similar trend was observed for each individual reaction for the  $K_{\text{i}}$  values: D-2HG > L-2HG > N-OG (Table 2). For the inhibition of AlkB-catalyzed reactions, there is no clear trend in the inhibitory potency between the D- and L-2HG; N-OG, however, is a stronger inhibitor than either of 2HG isomers. We also measured the  $\text{IC}_{50}$  of D- and L-2HG on the three enzymes (Table S7); in general, the  $\text{IC}_{50}$  values correlate well with the  $K_{\text{i}}$  values.

To make our experiments more relevant with regard to the anticipated cellular concentrations of metabolites/oncometabolites observed in human tumors, we also evaluated the extent inhibition of the ALKBH2 and ALKBH3 repair reactions by varying the ratios of D- or L-2HG to  $\alpha$ KG. For D-2HG inhibition, we tested a ratio of concentrations for D-2HG: $\alpha$ KG = 373:1, which was observed in glioma patients with IDH mutations (detailed information see the Discussion section).<sup>6</sup> The concentration of  $\alpha$ KG was fixed at 100  $\mu\text{M}$  to make sure that the kinetic analyses reflected steady state catalysis (Figure S5). We found that the repair efficiencies of ALKBH2 and ALKBH3 were 73–88% inhibited under such conditions, (Figure 3c, Table 3). For L-2HG inhibition, we tested a ratio of L-2HG: $\alpha$ KG = 28:1, which was reported in patients with kidney cancers (see Discussion section).<sup>10</sup> We found 48–58% of ALKBH2 and 31–40% of ALKBH3's activity was inhibited under this condition. These results suggest that the strong inhibition on DNA repair observed in the *in vitro* experiments may also occur in tumor cells of cancer patients.

## $\alpha$ KG Recovery of 2HG's Inhibition on the Repair Enzymes

Because 2-HG and  $\alpha$ KG are structurally similar, researchers hypothesized that 2HG is able to replace  $\alpha$ KG in the active site of  $\alpha$ KG dependent enzymes and competitively inhibit their enzymatic activities.<sup>7</sup> Crystal structures of histone demethylases show that D-2HG binds to the same site as  $\alpha$ KG in the catalytic center.<sup>7</sup> We tested the competition between 2HG and  $\alpha$ KG in the DNA repair reactions. Using ALKBH2 repair of m1A as an example, the repair ratios without adding 2HG were controlled to be around 60% under different  $\alpha$ KG concentrations (0.1, 0.5 and 1.0 mM, Figure 4 and Table S6). For the inhibition reactions, D-2HG was added at a fixed concentration (10 mM) in the reaction mixture, which contained ALKBH2 and necessary cofactors. Then, different concentrations of  $\alpha$ KG were added and mixed. After that the reaction was initiated by adding the oligonucleotide substrates. When 0.1 mM  $\alpha$ KG was present, the conversion decreased to 22%. When 0.5 mM and 1.0 mM  $\alpha$ KG were added, the repair ratio increased to 35% and 38%, respectively (Figure 4 and Table S6). This observed trend of reactivity recovery is consistent with the notion that D-2HG acts as a competitive inhibitor in the  $\alpha$ KG-dependent DNA repair reactions.<sup>7</sup> Similar recovery patterns were observed for all other D- and L-2HG inhibition reactions on all three enzymes (Figure 4 and Table S6).

## DISCUSSION

### Biological Implications of 2HG Inhibition of DNA Repair Enzymes

In the current study, we have shown that both D- and L-enantiomers of the oncometabolite 2HG can significantly inhibit the human DNA repair enzymes ALKBH2 and ALKBH3 under physiologically relevant concentrations. The concentrations of D-2HG and  $\alpha$ KG on average in glioma cells are 15.5  $\mu$ mol/g, and 0.0415  $\mu$ mol/g, respectively, which correspond to a concentration ratio between D-2HG and  $\alpha$ KG of 373 to 1,<sup>6,7</sup> Under this ratio condition, the repair activities of ALKBH2 and ALKBH3 were 73–88% inhibited (Table 3). The concentrations of L-2HG and  $\alpha$ KG on average in kidney cancer cells are 1.15  $\mu$ mol/g and 0.0484  $\mu$ mol/g, respectively, which corresponds to a concentration ratio between L-2HG and  $\alpha$ KG of 28 to 1.<sup>10</sup> Under this ratio condition, ALKBH2 and ALKBH3's repair activities are 31–58% inhibited (Table 3). Although the relative concentration of L-2HG (1.15  $\mu$ mol/g) is more than 10 times lower than D-2HG (15.5  $\mu$ mol/g), the ALKBH2 and ALKBH3 enzymes are still soundly inhibited by L-2HG partially due to the higher binding affinity of L-2HG (i.e., lower  $K_i$ ) than D-2HG (Table 2). The extent of inhibition in both cases was measured when the concentration of  $\alpha$ KG was fixed at 100  $\mu$ M, to ensure steady state catalysis. However, at lower concentrations of  $\alpha$ KG, (i.e., 50 or 20  $\mu$ M), the efficiency of adduct repair decreased even further. The cellular concentrations of  $\alpha$ KG are typically around 40 to 50  $\mu$ M (0.0415 and 0.0484  $\mu$ mol/g or mM) in cancer patients,<sup>6,10</sup> which are near to the 50–100  $\mu$ M range used in our experiments. Our data also show that, consistent with competitive inhibition of 2HG, the inhibition activity in the repair reaction reflects primarily the ratio between 2HG and  $\alpha$ KG. ALKBH2 and ALKBH3 are enzymes that repair alkyl DNA damage; hence, inhibition of DNA repair leads to alkylation product accumulation, less cellular survival, and increased mutations, which affect the resistance/sensitivity balance to alkylating chemotherapeutics. The elevation of both D- and L-2HG in cancer cells may contribute to the increased mutation rate and exacerbate tumorigenesis and progression.



## Strand Preference of the Three Repair Enzymes

According to the literature, ALKBH2 prefers to repair m1A and m3C in ds-DNA, whereas ALKBH3 and AlkB prefer to repair those adducts in ss-DNA.<sup>24,30,55</sup> We tested the repair activity in both ss-DNA and ds-DNA substrates in this study. The experimental results reported in this paper provide a strong kinetic basis for the previous observations. For ALKBH2, the  $k_{cat}/K_M$  values of ds-repair are higher than the repair in ss-DNA (Table 1). By contrast, the  $k_{cat}/K_M$  values of AlkB repair are higher for ss-DNA substrates than for ds-DNA substrates (Table 1). For ALKBH3, we were only able to measure the kinetic parameters for ss-repair, as the ds-repair reactions were too inefficient to evaluate. These results agree with and add quantitative detail to previous observations that ALKBH3 strongly prefers to repair adducts in ss-DNA.

## Other $\alpha$ KG/Fe(II)-Dependent Enzymes may be Inhibited by Oncometabolites

There are about 80 proteins in the  $\alpha$ KG/Fe(II)-dependent enzyme family, including jmjc, prolyl hydroxylase, TET, and the AlkB family enzymes.<sup>21–23</sup> Studies have demonstrated that D- and L-2HG inhibit jmjc and TET family proteins.<sup>7,62</sup> In addition to 2HG, intermediates in the TCA cycle such as succinate and fumarate have also been found to exhibit higher-than-normal concentrations in different cancer cells (Figure 1b).<sup>18</sup> Given their structural similarities to  $\alpha$ KG and 2HG, these metabolites could also perturb  $\alpha$ KG-dependent enzymatic activities in the cell, especially DNA repair processes that are related to the AlkB family enzymes. Systematic studies are needed to explore these possibilities and correlate these biochemical results with clinical observations. These studies are also pivotal for the design and development of therapeutic agents that target the abnormal metabolic pathways of cancer.

## Supplementary Material

Refer to Web version on PubMed Central for supplementary material.

## Acknowledgments

### Funding Sources

This work was supported by an Institutional Development Award from the National Institute of General Medical Sciences of the National Institutes of Health under grant number 2 P20 GM103430, and a Medical Research Funds grant from the Rhode Island foundation (to D. L.). This work was also supported, in whole or in part, by National Institutes of Health Grants P01 CA26731, R01 CA080024, and P30 ES002109 (to J.M.E.).

The authors want to thank the RI-INBRE program, its directors Prof. Zahir Shaikh and Prof. David Rowley, and staff Dr. Al Bach, Ms. Kim Andrews and Ms. Patricia Murray for their kind help. We also want to thank Prof. Bongsup Cho, Prof. Roberta King, Mr. Aram Babcock, and Mr. Ang Cai for their support and helpful discussions.

## ABBREVIATIONS

<b>m1A</b>	1-methyladenine
<b>m3C</b>	3-methylcytosine
<b>ESI</b>	electrospray ionization

<b>TOF</b>	time-of-flight
<b>MS</b>	mass spectrometry
<b>ss</b>	single stranded
<b>ds</b>	double stranded

## References

1. Yan H, Parsons DW, Jin G, McLendon R, Rasheed BA, Yuan W, Kos I, Batinic-Haberle I, Jones S, Riggins GJ, Friedman H, Friedman A, Reardon D, Herndon J, Kinzler KW, Velculescu VE, Vogelstein B, Bigner DD. IDH1 and IDH2 mutations in gliomas. *N. Engl. J. Med.* 2009; 360:765–773. [PubMed: 19228619]
2. Parsons DW, Jones S, Zhang X, Lin JC-H, Leary RJ, Angenendt P, Mankoo P, Carter H, Siu I-M, Gallia GL, Olivi A, McLendon R, Rasheed BA, Keir S, Nikolskaya T, Nikolsky Y, Busam DA, Tekleab H, Diaz LA, Hartigan J, Smith DR, Strausberg RL, Marie SKN, Shinjo SMO, Yan H, Riggins GJ, Bigner DD, Karchin R, Papadopoulos N, Parmigiani G, Vogelstein B, Velculescu VE, Kinzler KW. An integrated genomic analysis of human glioblastoma multiforme. *Science.* 2008; 321:1807–1812. [PubMed: 18772396]
3. Mardis ER, Ding L, Dooling DJ, Larson DE, McLellan MD, Chen K, Koboldt DC, Fulton RS, Delehaunty KD, McGrath SD, Fulton LA, Locke DP, Magrini VJ, Abbott RM, Vickery TL, Reed JS, Robinson JS, Wylie T, Smith SM, Carmichael L, Eldred JM, Harris CC, Walker J, Peck JB, Du F, Dukes AF, Sanderson GE, Brummett AM, Clark E, McMichael JF, Meyer RJ, Schindler JK, Pohl CS, Wallis JW, Shi X, Lin L, Schmidt H, Tang Y, Haipek C, Wiechert ME, Ivy JV, Kalicki J, Elliott G, Ries RE, Payton JE, Westervelt P, Tomasson MH, Watson MA, Baty J, Heath S, Shannon WD, Nagarajan R, Link DC, Walter MJ, Graubert TA, DiPersio JF, Wilson RK, Ley TJ. Recurring mutations found by sequencing an acute myeloid leukemia genome. *N. Engl. J. Med.* 2009; 361:1058–1066. [PubMed: 19657110]
4. Yang H, Ye D, Guan K-L, Xiong Y. IDH1 and IDH2 mutations in tumorigenesis: mechanistic insights and clinical perspectives. *Clin. Cancer Res. Off. J. Am. Assoc. Cancer Res.* 2012; 18:5562–5571.
5. Cairns RA, Mak TW. Oncogenic isocitrate dehydrogenase mutations: mechanisms, models, and clinical opportunities. *Cancer Discov.* 2013; 3:730–741. [PubMed: 23796461]
6. Dang L, White DW, Gross S, Bennett BD, Bittinger MA, Driggers EM, Fantin VR, Jang HG, Jin S, Keenan MC, Marks KM, Prins RM, Ward PS, Yen KE, Liao LM, Rabinowitz JD, Cantley LC, Thompson CB, Vander Heiden MG, Su SM. Cancer-associated IDH1 mutations produce 2-hydroxyglutarate. *Nature.* 2009; 462:739–744. [PubMed: 19935646]
7. Xu W, Yang H, Liu Y, Yang Y, Wang P, Kim S-H, Ito S, Yang C, Wang P, Xiao M-T, Liu L, Jiang W, Liu J, Zhang J, Wang B, Frye S, Zhang Y, Xu Y, Lei Q, Guan K-L, Zhao S, Xiong Y. Oncometabolite 2-hydroxyglutarate is a competitive inhibitor of  $\alpha$ -ketoglutarate-dependent dioxygenases. *Cancer Cell.* 2011; 19:17–30. [PubMed: 21251613]
8. Chowdhury R, Yeoh KK, Tian Y-M, Hillringhaus L, Bagg EA, Rose NR, Leung IKH, Li XS, Woon EY, Yang M, McDonough MA, King ON, Clifton IJ, Klose RJ, Claridge TDW, Ratcliffe PJ, Schofield CJ, Kawamura A. The oncometabolite 2-hydroxyglutarate inhibits histone lysine demethylases. *EMBO Rep.* 2011; 12:463–469. [PubMed: 21460794]
9. Shim E-H, Sudarshan S. Another small molecule in the oncometabolite mix: L-2-Hydroxyglutarate in kidney cancer. *OncoScience.* 2015; 2:483–486. [PubMed: 26097881]
10. Shim E-H, Livi CB, Rakheja D, Tan J, Benson D, Parekh V, Kho E-Y, Ghosh AP, Kirkman R, Velu S, Dutta S, Chenna B, Rea SL, Mishur RJ, Li Q, Johnson-Pais TL, Guo L, Bae S, Wei S, Block K, Sudarshan S. L-2-Hydroxyglutarate: an epigenetic modifier and putative oncometabolite in renal cancer. *Cancer Discov.* 2014; 4:1290–1298. [PubMed: 25182153]
11. Oldham WM, Clish CB, Yang Y, Loscalzo J. Hypoxia-mediated increases in L-2-hydroxyglutarate coordinate the metabolic response to reductive stress. *Cell Metab.* 2015; 22:291–303. [PubMed: 26212716]

12. Intlekofer AM, Dematteo RG, Venneti S, Finley LWS, Lu C, Judkins AR, Rustenburg AS, Grinaway PB, Chodera JD, Cross JR, Thompson CB. Hypoxia induces production of L-2-hydroxyglutarate. *Cell Metab.* 2015; 22:304–311. [PubMed: 26212717]
13. Armitage EG, Kotze HL, Allwood JW, Dunn WB, Goodacre R, Williams KJ. Metabolic profiling reveals potential metabolic markers associated with hypoxia inducible factor-mediated signalling in hypoxic cancer cells. *Sci. Rep.* 2015; 5:15649. [PubMed: 26508589]
14. Worth AJ, Gillespie KP, Mesaros C, Guo L, Basu SS, Snyder NW, Blair IA. Rotenone stereospecifically increases (S)-2-hydroxyglutarate in SH-SY5Y neuronal cells. *Chem. Res. Toxicol.* 2015; 28:948–954. [PubMed: 25800467]
15. Vatrinet R, Leone G, De Luise M, Girolimetti G, Vidone M, Gasparre G, Porcelli AM. The  $\alpha$ -ketoglutarate dehydrogenase complex in cancer metabolic plasticity. *Cancer Metab.* 2017; 5:3. [PubMed: 28184304]
16. Pavlova NN, Thompson CB. The emerging hallmarks of cancer metabolism. *Cell Metab.* 2016; 23:27–47. [PubMed: 26771115]
17. Hirschev MD, DeBerardinis RJ, Diehl AME, Drew JE, Frezza C, Green MF, Jones LW, Ko YH, Le A, Lea MA, Locasale JW, Longo VD, Lyssiotis CA, McDonnell E, Mehrmohamadi M, Michelotti G, Muralidhar V, Murphy MP, Pedersen PL, Poore B, Raffaghello L, Rathmell JC, Sivanand S, Vander Heiden MG, Wellen KE. Target Validation Team. Dysregulated metabolism contributes to oncogenesis. *Semin. Cancer Biol.* 2015; 35:S129–150. [PubMed: 26454069]
18. Nowicki S, Gottlieb E. Oncometabolites: tailoring our genes. *FEBS J.* 2015; 282:2796–2805. [PubMed: 25864878]
19. Gaude E, Frezza C. Defects in mitochondrial metabolism and cancer. *Cancer Metab.* 2014; 2:10. [PubMed: 25057353]
20. Su X, Wellen KE, Rabinowitz JD. Metabolic control of methylation and acetylation. *Curr. Opin. Chem. Biol.* 2016; 30:52–60. [PubMed: 26629854]
21. Markolovic S, Wilkins SE, Schofield CJ. Protein hydroxylation catalyzed by 2-oxoglutarate-dependent oxygenases. *J. Biol. Chem.* 2015; 290:20712–20722. [PubMed: 26152730]
22. Hausinger, RP., Schofield, CJ., editors. 2-Oxoglutarate-dependent oxygenases. Royal Society of Chemistry; Cambridge, UK: 2015.
23. Martinez S, Hausinger RP. Catalytic mechanisms of Fe(II)- and 2-oxoglutarate-dependent oxygenases. *J. Biol. Chem.* 2015; 290:20702–20711. [PubMed: 26152721]
24. Fedeles BI, Singh V, Delaney JC, Li D, Essigmann JM. The AlkB family of Fe(II)/ $\alpha$ -ketoglutarate-dependent dioxygenases: repairing nucleic acid alkylation damage and beyond. *J. Biol. Chem.* 2015; 290:20734–20742. [PubMed: 26152727]
25. Wang P, Wu J, Ma S, Zhang L, Yao J, Hoadley KA, Wilkerson MD, Perou CM, Guan K-L, Ye D, Xiong Y. Oncometabolite D-2-hydroxyglutarate inhibits ALKBH DNA repair enzymes and sensitizes IDH mutant cells to alkylating agents. *Cell Rep.* 2015; 13:2353–2361. [PubMed: 26686626]
26. Johannessen T-CA, Prestegarden L, Grudic A, Hegi ME, Tysnes BB, Bjerkvig R. The DNA repair protein ALKBH2 mediates temozolomide resistance in human glioblastoma cells. *Neuro-Oncol.* 2013; 15:269–278. [PubMed: 23258843]
27. Trewick SC, Henshaw TF, Hausinger RP, Lindahl T, Sedgwick B. Oxidative demethylation by *Escherichia coli* AlkB directly reverts DNA base damage. *Nature.* 2002; 419:174–178. [PubMed: 12226667]
28. Falnes PØ, Johansen RF, Seeberg E. AlkB-mediated oxidative demethylation reverses DNA damage in *Escherichia coli*. *Nature.* 2002; 419:178–182. [PubMed: 12226668]
29. Aravind L, Koonin EV. The DNA-repair protein AlkB, EGL-9, and leprecan define new families of 2-oxoglutarate- and iron-dependent dioxygenases. *Genome Biol.* 2001; 2:RESEARCH0007. [PubMed: 11276424]
30. Sedgwick B, Bates PA, Paik J, Jacobs SC, Lindahl T. Repair of alkylated DNA: recent advances. *DNA Repair.* 2007; 6:429–442. [PubMed: 17112791]
31. Fu D, Samson LD. Direct repair of 3,N(4)-ethenocytosine by the human ALKBH2 dioxygenase is blocked by the AAG/MPG glycosylase. *DNA Repair.* 2012; 11:46–52. [PubMed: 22079122]

32. Li P, Gao S, Wang L, Yu F, Li J, Wang C, Li J, Wong J. ABH2 couples regulation of ribosomal DNA transcription with DNA alkylation repair. *Cell Rep.* 2013; 4:817–829. [PubMed: 23972994]
33. Chen B, Liu H, Sun X, Yang C-G. Mechanistic insight into the recognition of single-stranded and double-stranded DNA substrates by ABH2 and ABH3. *Mol. Biosyst.* 2010; 6:2143–2149. [PubMed: 20714506]
34. Yang C-G, Yi C, Duguid EM, Sullivan CT, Jian X, Rice PA, He C. Crystal structures of DNA/RNA repair enzymes AlkB and ABH2 bound to dsDNA. *Nature.* 2008; 452:961–965. [PubMed: 18432238]
35. Yi C, Jia G, Hou G, Dai Q, Zhang W, Zheng G, Jian X, Yang C-G, Cui Q, He C. Iron-catalysed oxidation intermediates captured in a DNA repair dioxygenase. *Nature.* 2010; 468:330–333. [PubMed: 21068844]
36. Nay SL, Lee D-H, Bates SE, O'Connor TR. Alkhh2 protects against lethality and mutation in primary mouse embryonic fibroblasts. *DNA Repair.* 2012; 11:502–510. [PubMed: 22429847]
37. Dango S, Mosammaparast N, Sowa ME, Xiong L-J, Wu F, Park K, Rubin M, Gygi S, Harper JW, Shi Y. DNA unwinding by ASCC3 helicase is coupled to ALKBH3-dependent DNA alkylation repair and cancer cell proliferation. *Mol. Cell.* 2011; 44:373–384. [PubMed: 22055184]
38. Koike K, Ueda Y, Hase H, Kitae K, Fusamae Y, Masai S, Inagaki T, Saigo Y, Hirasawa S, Nakajima K, Ohshio I, Makino Y, Konishi N, Yamamoto H, Tsujikawa K. Anti-tumor effect of AlkB homolog 3 knockdown in hormone-independent prostate cancer cells. *Curr. Cancer Drug Targets.* 2012; 12:847–856. [PubMed: 22515525]
39. Calvo JA, Meira LB, Lee C-YI, Moroski-Erkul CA, Abolhassani N, Taghizadeh K, Eichinger LW, Muthupalani S, Nordstrand LM, Klungland A, Samson LD. DNA repair is indispensable for survival after acute inflammation. *J. Clin. Invest.* 2012; 122:2680–2689. [PubMed: 22684101]
40. Sundheim O, Vågbø CB, Bjørås M, Sousa MML, Talstad V, Aas PA, Drabløs F, Krokan HE, Tainer JA, Slupphaug G. Human ABH3 structure and key residues for oxidative demethylation to reverse DNA/RNA damage. *EMBO J.* 2006; 25:3389–3397. [PubMed: 16858410]
41. Li D, Fedeles BI, Shrivastav N, Delaney JC, Yang X, Wong C, Drennan CL, Essigmann JM. Removal of N-alkyl modifications from N(2)-alkylguanine and N(4)-alkylcytosine in DNA by the adaptive response protein AlkB. *Chem. Res. Toxicol.* 2013; 26:1182–1187. [PubMed: 23773213]
42. Maciejewska AM, Poznanski J, Kaczmarek Z, Krowisz B, Nieminuszczy J, Polkowska-Nowakowska A, Grzesiuk E, Kusmierk JT. AlkB dioxygenase preferentially repairs protonated substrates: specificity against exocyclic adducts and molecular mechanism of action. *J. Biol. Chem.* 2013; 288:432–441. [PubMed: 23148216]
43. Delaney JC, Essigmann JM. Mutagenesis, genotoxicity, and repair of 1-methyladenine, 3-alkylcytosines, 1-methylguanine, and 3-methylthymine in alkB *Escherichia coli*. *Proc. Natl. Acad. Sci. U. S. A.* 2004; 101:14051–14056. [PubMed: 15381779]
44. Delaney JC, Smeester L, Wong C, Frick LE, Taghizadeh K, Wishnok JS, Drennan CL, Samson LD, Essigmann JM. AlkB reverses etheno DNA lesions caused by lipid oxidation *in vitro* and *in vivo*. *Nat. Struct. Mol. Biol.* 2005; 12:855–860. [PubMed: 16200073]
45. Frick LE, Delaney JC, Wong C, Drennan CL, Essigmann JM. Alleviation of 1,N6-ethanoadenine genotoxicity by the *Escherichia coli* adaptive response protein AlkB. *Proc. Natl. Acad. Sci. U. S. A.* 2007; 104:755–760. [PubMed: 17213319]
46. Li D, Delaney JC, Page CM, Chen AS, Wong C, Drennan CL, Essigmann JM. Repair of DNA alkylation damage by the *Escherichia coli* adaptive response protein AlkB as studied by ESI-TOF mass spectrometry. *J. Nucleic Acids.* 2010; 369434. [PubMed: 21048928]
47. Li D, Delaney JC, Page CM, Yang X, Chen AS, Wong C, Drennan CL, Essigmann JM. Exocyclic carbons adjacent to the N6 of adenine are targets for oxidation by the *Escherichia coli* adaptive response protein AlkB. *J. Am. Chem. Soc.* 2012; 134:8896–8901. [PubMed: 22512456]
48. Singh V, Fedeles BI, Li D, Delaney JC, Kozekov ID, Kozekova A, Marnett LJ, Rizzo CJ, Essigmann JM. Mechanism of repair of acrolein- and malondialdehyde-derived exocyclic guanine adducts by the  $\alpha$ -ketoglutarate/Fe(II) dioxygenase AlkB. *Chem. Res. Toxicol.* 2014; 27:1619–1631. [PubMed: 25157679]
49. Chang S, Fedeles BI, Wu J, Delaney JC, Li D, Zhao L, Christov PP, Yau E, Singh V, Jost M, Drennan CL, Marnett LJ, Rizzo CJ, Levine SS, Guengerich FP, Essigmann JM. Next-generation

- sequencing reveals the biological significance of the N(2),3-ethenoguanine lesion *in vivo*. *Nucleic Acids Res.* 2015; 43:5489–5500. [PubMed: 25837992]
50. Yi C, He C. DNA repair by reversal of DNA damage. *Cold Spring Harb. Perspect. Biol.* 2013; 5:a012575. [PubMed: 23284047]
51. Ougland R, Rognes T, Klungland A, Larsen E. Non-homologous functions of the AlkB homologs. *J. Mol. Cell Biol.* 2015; 7:494–504. [PubMed: 26003568]
52. Fu D, Calvo JA, Samson LD. Balancing repair and tolerance of DNA damage caused by alkylating agents. *Nat. Rev. Cancer.* 2012; 12:104–120. [PubMed: 22237395]
53. Shrivastav N, Li D, Essigmann JM. Chemical biology of mutagenesis and DNA repair: cellular responses to DNA alkylation. *Carcinogenesis.* 2010; 31:59–70. [PubMed: 19875697]
54. Zheng G, Fu Y, He C. Nucleic acid oxidation in DNA damage repair and epigenetics. *Chem. Rev.* 2014; 114:4602–4620. [PubMed: 24580634]
55. Chen F, Tang Q, Bian K, Humulock ZT, Yang X, Jost M, Drennan CL, Essigmann JM, Li D. Adaptive response enzyme AlkB preferentially repairs 1-methylguanine and 3-methylthymine adducts in double-stranded DNA. *Chem. Res. Toxicol.* 2016; 29:687–693. [PubMed: 26919079]
56. Zhu C, Yi C. Switching demethylation activities between AlkB family RNA/DNA demethylases through exchange of active-site residues. *Angew. Chem. Int. Ed Engl.* 2014; 53:3659–3662. [PubMed: 24596302]
57. Ehrismann D, Flashman E, Genn DN, Mathioudakis N, Hewitson KS, Ratcliffe PJ, Schofield CJ. Studies on the activity of the hypoxia-inducible-factor hydroxylases using an oxygen consumption assay. *Biochem. J.* 2007; 401:227–234. [PubMed: 16952279]
58. Ergel B, Gill ML, Brown L, Yu B, Palmer AG, Hunt JF. Protein dynamics control the progression and efficiency of the catalytic reaction cycle of the *Escherichia coli* DNA-repair enzyme AlkB. *J. Biol. Chem.* 2014; 289:29584–29601. [PubMed: 25043760]
59. Lee D-H, Jin S-G, Cai S, Chen Y, Pfeifer GP, O'Connor TR. Repair of methylation damage in DNA and RNA by mammalian AlkB homologues. *J. Biol. Chem.* 2005; 280:39448–39459. [PubMed: 16174769]
60. Roy TW, Bhagwat AS. Kinetic studies of *Escherichia coli* AlkB using a new fluorescence-based assay for DNA demethylation. *Nucleic Acids Res.* 2007; 35:e147. [PubMed: 18003660]
61. Yu B, Hunt JF. Enzymological and structural studies of the mechanism of promiscuous substrate recognition by the oxidative DNA repair enzyme AlkB. *Proc. Natl. Acad. Sci. U. S. A.* 2009; 106:14315–14320. [PubMed: 19706517]
62. Figueroa ME, Abdel-Wahab O, Lu C, Ward PS, Patel J, Shih A, Li Y, Bhagwat N, Vasanthakumar A, Fernandez HF, Tallman MS, Sun Z, Wolniak K, Peeters JK, Liu W, Choe SE, Fantin VR, Paietta E, Löwenberg B, Licht JD, Godley LA, Delwel R, Valk PJM, Thompson CB, Levine RL, Melnick A. Leukemic IDH1 and IDH2 mutations result in a hypermethylation phenotype, disrupt TET2 function, and impair hematopoietic differentiation. *Cancer Cell.* 2010; 18:553–567. [PubMed: 21130701]

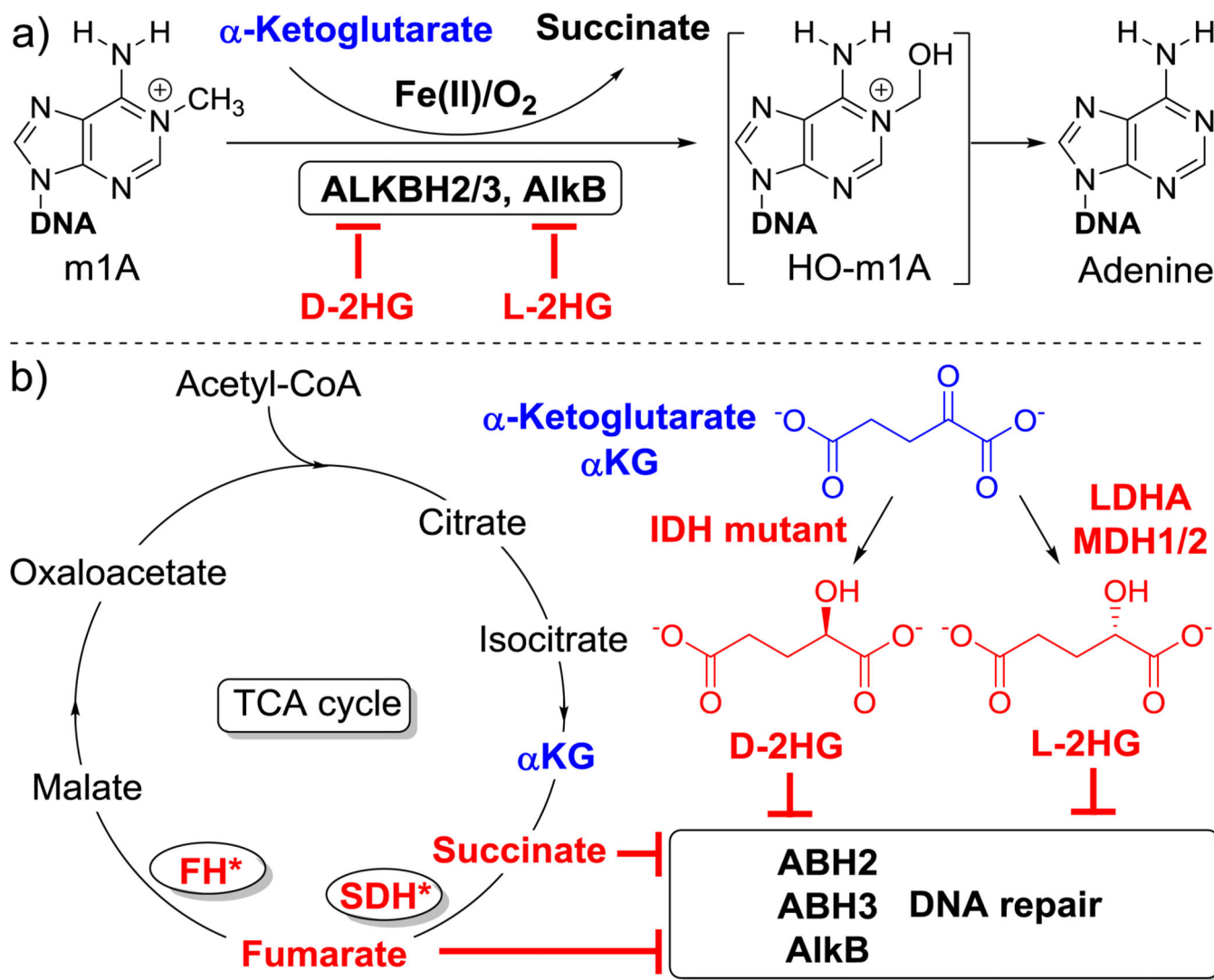


**Figure 1.**

a) Repair mechanism of the AlkB family enzymes on alkyl DNA lesions. Adduct m1A is used here as an example to show the steps of enzymatic catalysis. b) The generation of D- and L-2HG and mechanisms of inhibition to the AlkB family DNA repair enzymes.

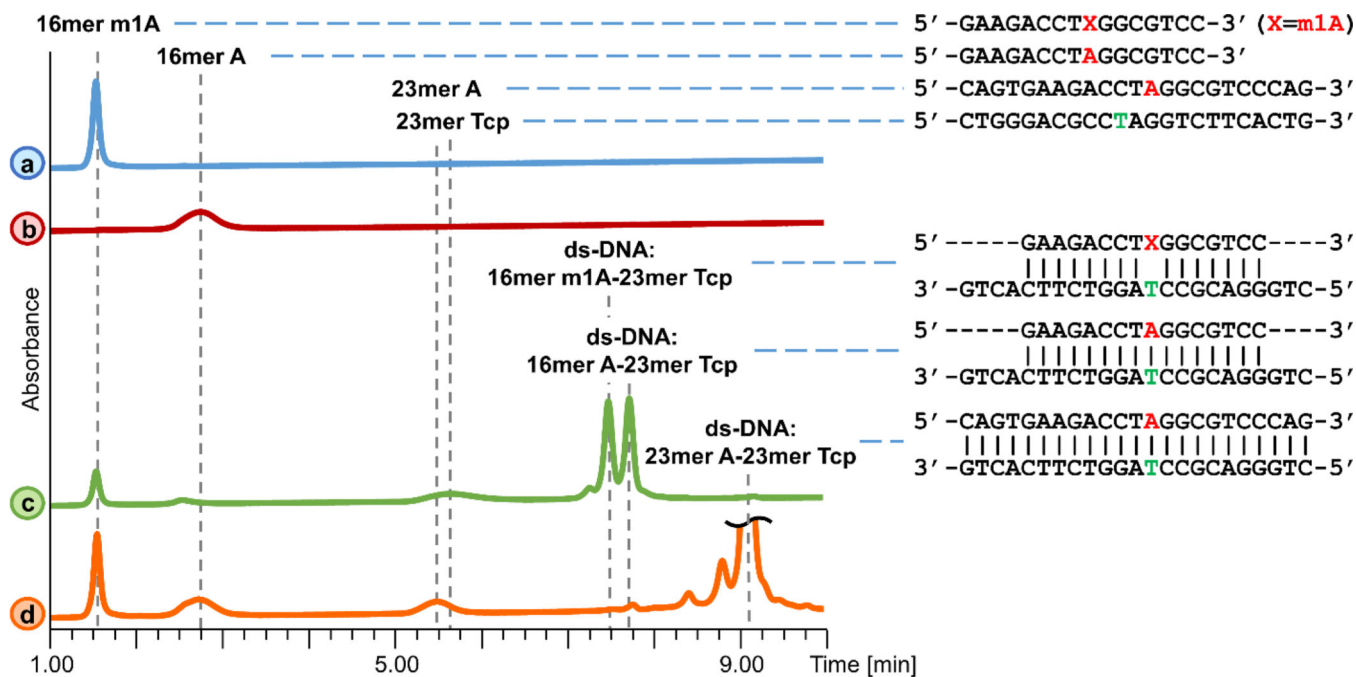


**Figure 2.**

HPLC analyses of the DNA repair reactions. a) Starting material 16mer oligonucleotide containing m1A at the lesion site in ss-DNA reaction. b) ss-Product 16mer oligonucleotide containing A at the “lesion site” in the ss-DNA reaction. c) ds-DNA reaction products of 16mer m1A with 23mer Tcp. The mixture containing ss-16mer m1A, ss-16mer A, ds-16mer m1A:23mer Tcp, and ds-16mer A:23mer Tcp. The latter two species were not fully separable by HPLC. d) ds-DNA reaction products of 16mer m1 A with 23mer Tcp and additional 23mer A, which is fully complementary to 23mer Tcp. The duplex of 23mer Tcp: 23mer A was eluted as ds-DNA, thus releasing ss-16mer m1A and ss-16mer A for quantification.

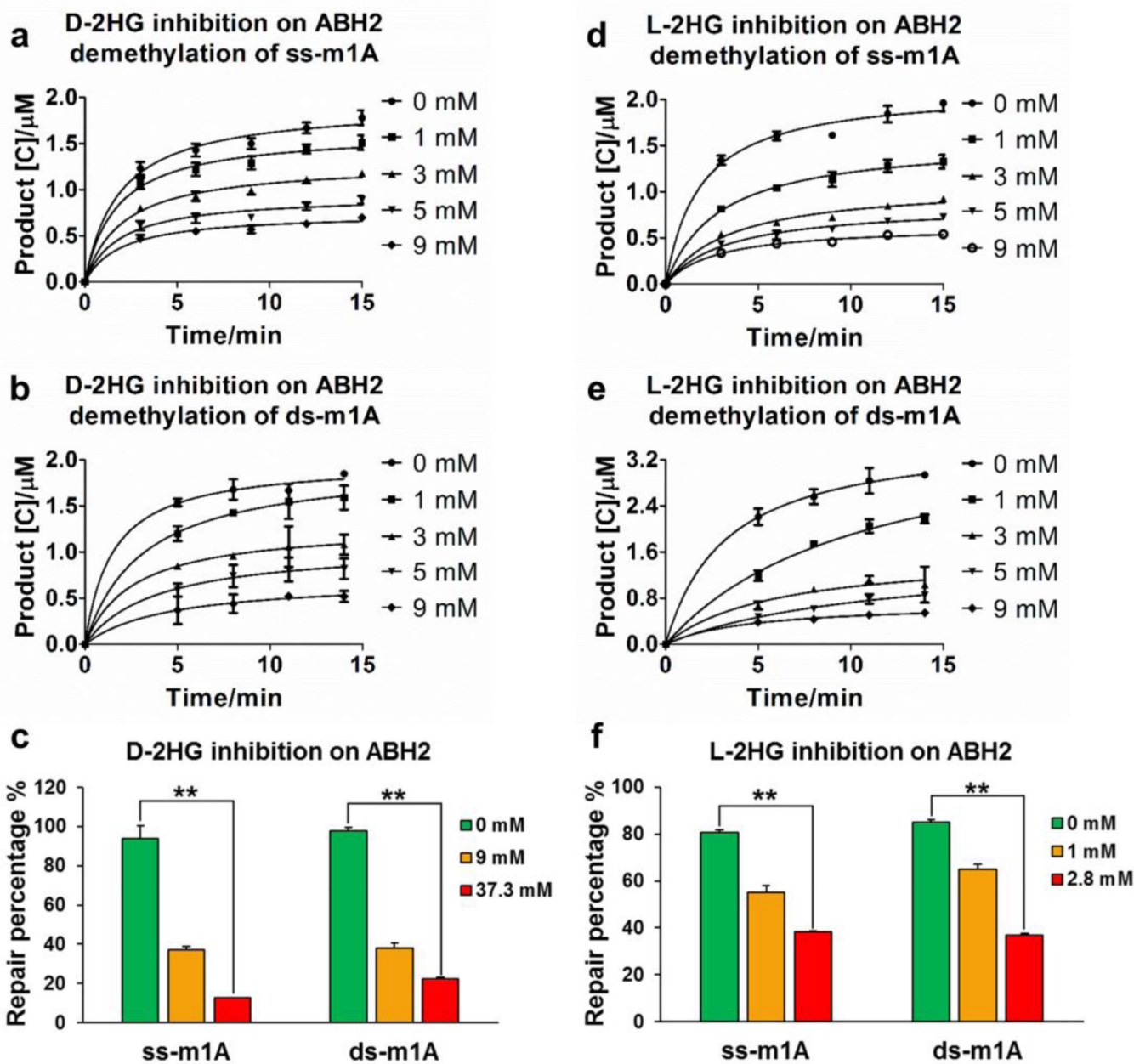


**Figure 3.** Inhibition of ALKBH2 repair of ml A in ss- and ds-DNA by D- and L-2HG. a) Inhibition of D-2HG on ml A repair in ss-DNA. b) Inhibition of D-2HG on ml A repair in ds-DNA. c) Inhibition of D-2HG on ml A repair under D-2HG: $\alpha$ KG = 373:1 ratio conditions, d) Inhibition of L-2HG on ml A repair in ss-DNA. e) Inhibition of L-2HG on ml A repair in ds-DNA. f) Inhibition of L-2HG on ml A repair under L-2HG: $\alpha$ KG = 28:1 ratio conditions.



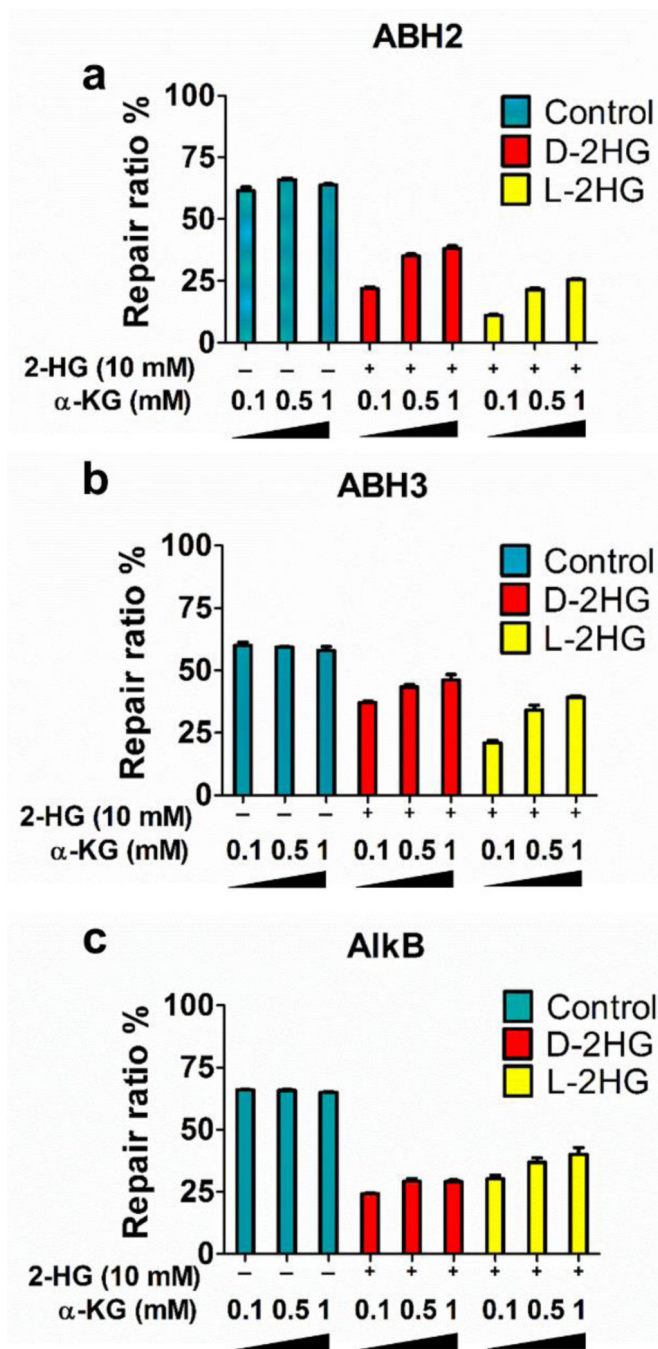


**Figure 4.** Addition of  $\alpha$ KG reverses the inhibitory effect of 2-HG toward ALKBH2 repair of ml A. Different concentrations of  $\alpha$ KG were added to a fixed concentration of 2HG (10 mM) to recover the repair of ml A by a) ALKBH2, b) ALKBH3 and c) AlkB.

**Table 1**Kinetic constants of  $\alpha$ KG as a substrate on ALKBH2, ALKBH3 and AlkB repair reactions.

Enzyme	Condition	$K_M$ [ $\mu$ M]	$k_{cat}$ [ $\text{min}^{-1}$ ]	$\frac{k_{cat}}{K_M}$ [ $\text{min}^{-1}\cdot\mu\text{M}^{-1}$ ]
ALKBH2	ss-m1A	$4.1 \pm 0.9$	$1.1 \pm 0.1$	0.28
	ds-m1A	$7.3 \pm 0.9$	$2.5 \pm 0.1$	0.34
	ss-m3C	$1.4 \pm 0.2$	$1.7 \pm 0.1$	1.20
	ds-m3C	$1.9 \pm 0.4$	$2.6 \pm 0.1$	1.34
ALKBH3	ss-m1A	$2.3 \pm 0.1$	$1.2 \pm 0.0$	0.51
	ss-m3C	$1.9 \pm 0.4$	$1.7 \pm 0.0$	0.87
AlkB	ss-m1A	$7.1 \pm 1.1$	$4.2 \pm 0.2$	0.59
	ds-m1A	$12.7 \pm 1.3$	$4.8 \pm 0.2$	0.38
	ss-m3C	$19.9 \pm 1.3$	$24.5 \pm 0.7$	1.23
	ds-m3C	$10.8 \pm 1.9$	$8.2 \pm 0.4$	0.76

**Table 2**

Inhibition constant ( $K_i$ ) of D-2HG, L-2HG and N-OG. The individual inhibition reactions were depicted in Figure S6 to S15.

Enzyme	Condition	$K_i$ [ $\mu$ M]		
		D-2HG	L-2HG	N-OG
ALKBH2	ss-m1A	405 $\pm$ 61	275 $\pm$ 41	30 $\pm$ 7
	ds-m1A	280 $\pm$ 61	180 $\pm$ 36	16 $\pm$ 5
	ss-m3C	152 $\pm$ 13	64 $\pm$ 3	40 $\pm$ 7
	ds-m3C	79 $\pm$ 11	76 $\pm$ 11	7 $\pm$ 2
ALKBH3	ss-m1A	545 $\pm$ 77	185 $\pm$ 23	27 $\pm$ 4
	ss-m3C	490 $\pm$ 46	228 $\pm$ 16	37 $\pm$ 3
AlkB	ss-m1A	571 $\pm$ 166	337 $\pm$ 99	0.4 $\pm$ 0.1
	ds-m1A	529 $\pm$ 126	598 $\pm$ 173	2.0 $\pm$ 1.3
	ss-m3C	447 $\pm$ 113	276 $\pm$ 111	0.4 $\pm$ 0.1
	ds-m3C	230 $\pm$ 55	308 $\pm$ 108	0.2 $\pm$ 0.0

**Table 3**Inhibition ratio of D-2HG (373 fold to  $\alpha$ KG) and L-2HG (28 fold to  $\alpha$ KG) on ALKBH2 and ALKBH3.

Enzyme	Condition	% Inhibition of 373-fold D-2H to $\alpha$ KG	% Inhibition of 28-fold L-2HG to $\alpha$ KG
ALKBH2	ss-m1A	86	53
	ds-m1A	77	57
	ss-m3C	88	48
	ds-m3C	88	58
ALKBH3	ss-m1A	80	40
	ds-m1A	81	37
	ss-m3C	73	32
	ds-m3C	87	31